ORIGINAL ARTICLES

Molecular profiling of individual tumor cells by hyperspectral microscopic imaging

JONATHAN W. UHR, MICHAEL L. HUEBSCHMAN, EUGENE P. FRENKEL, NANCY L. LANE, RAHEELA ASHFAQ, HUAYING LIU, DIPEN R. RANA, LAWRENCE CHENG, ALICE T. LIN, GARETH A. HUGHES, XIAOJING J. ZHANG, and HAROLD R. GARNER

DALLAS AND AUSTIN, TX

We developed a hyperspectral microscopic imaging (HMI) platform that can precisely identify and quantify 10 molecular markers in individual cancer cells in a single pass. The exploitation of an improved separation of circulating tumor cells and the application of HMI provided an opportunity (1) to identify molecular changes in these cells, (2) to recognize the coexpression of these markers, (3) to pose an important opportunity for noninvasive diagnosis, and (4) to use targeted therapy. We balanced the intensity of 10 fluorochromes bound to 10 different antibodies, each specific to a particular tumor marker, so that the intensity of each fluorochrome can be discerned from overlapping emissions. Using 2 touch preps from each primary breast cancer, the average molecular marker intensities of 25 tumor cells gave a representative molecular signature for the tumor despite some cellular heterogeneity. The intensities determined by the HMI correlate well with the conventional 0–3+ analysis by experts in cellular pathology. Because additional multiplexes can be developed using the same fluorochromes but different antibodies, this analysis allows quantification of many molecular markers on a population of tumor cells. HMI can be automated completely, and eventually, it could allow the standardization of protein biomarkers and improve reproducibility among clinical pathology laboratories. (Translational Research 2012;159:366–375)

Abbreviations: 2D = 2-dimensional; 3D = 3-dimensional; CCD = charge-coupled device; CD = clusters of differentiation; CTC = circulating tumor cell; DAPI = 4′,6-diamidino-2-phenylindole; ER = estrogen receptor; HER2 = human epidermal growth factor receptor 2; HMI = hyperspectral microscopic imaging; IDL = Interactive Data Language; IgG = immunoglobulin G; ITC = individual tumor cell; PR = progesterone receptor; TC = tumor cell; uPAR = urokinase plasminogen activator receptor

From the Cancer Immunobiology Center, Department of Internal Medicine, at the University of Texas Southwestern Medical Center, Dallas, TX; McDermott Center for Human Growth and Development, Department of Internal Medicine, at the University of Texas Southwestern Medical Center, Dallas, TX; Harold C. Simmons Cancer Center, Department of Internal Medicine, at the University of Texas Southwestern Medical Center, Dallas, TX; Lynntech Inc, Dallas, TX; College of Engineering, University of Texas at Austin, Austin, TX.

Supported by the Raymond and Ellen Willie Distinguished Chair in Cancer Research (to J.U.), Grant 1RO1CA106272-01A1 from the National Cancer Institute, P.O'B, by Montgomery Distinguished Chair (to H.R.G.), the Hudson Foundation, the Texas Ignition Fund, the Nasher Family Cancer Research Program, and the T. Boone Pickens Fund.

Submitted for publication May 19, 2011; revision submitted August 5, 2011; accepted for publication August 8, 2011.

Reprint requests: Michael L. Huebschman, PhD, Department of Internal Medicine, Harold C. Simmons Comprehensive Cancer Center, 6000 Harry Hines Blvd, Dallas, TX 75390-8576; e-mail: michael.huebschman@utsouthwestern.edu.

1931-5244/$ - see front matter

doi:10.1016/j.trsl.2011.08.003

AT A GLANCE COMMENTARY

Uhr J, et al.

Background

Protein biomarkers and genomic alterations in primary cancers have been shown to predict the response to treatment and determine prognosis. Identification of pivotal genomic alterations that can be targeted is exemplified by treatment of HER2 overexpressing cancers with the anti-HER2 monoclonal antibody trastuzumab. Multiparametric analysis at the single-cell level allows characterization of many proteins and signaling pathways that generate particular phenotypes.

Translational Significance

Improved capture of circulating tumor cells and hyperspectral microscopic imaging facilitate identification and quantification of many molecular markers in cells at different times, recognition of co-expression of markers, and, thereby, allow non-invasive diagnosis and improved targeted therapy.

The paradigm of cancer treatment has emphasized the need for extensive molecular profiling of the cancer. The recognition of protein biomarkers and genomic alterations in primary cancers has been shown to predict response to treatment (predictive markers)[1,2] and determine prognosis.[3-5] The identification of pivotal genomic alterations that can be targeted is exemplified by the treatment of human epidermal growth factor receptor 2 (HER2) oncoprotein overexpressing cancers with the anti-HER2 monoclonal antibody trastuzumab.[6,7] The success of this strategy resulted in an intensive effort to understand cancer biology at a systems level. Multiparametric analysis at the single cell level is a technical hurdle that if crossed successfully could allow for the analysis of systematic (nonrandom) heterogeneity and could be informative of proteins and pathways that cooperate to generate specific phenotypes. Such information should facilitate the development of new targeted drugs and rationally designed combinations that intervene in defined signaling pathways to affect the natural progression of cancer, thus advancing the practice of truly individualized/personalized cancer therapy.

Using hyperspectral microscopic imaging (HMI) in this study, we present evidence that expansion and quantification of molecular signatures can be obtained on individual tumor cells (ITCs) stained with a panel of antibody-fluor conjugates that detect and quantify biomarkers of interest. The cells were obtained by touch preps of tumor tissue, capture of circulating tumor cells (CTCs), and by the use of cells from established cell lines. The result is an ability to analyze a large number of molecular markers on individual tumor cells and quantify their expression objectively and precisely. Clinical studies are in progress to define the level of expression of individual markers as well as nonrandom patterns of molecular markers within ITCs for correlative delineation of prognostic and/or predictive relevance.

MATERIALS AND METHODS

Hyperspectral microscopic imaging. An analysis of normal and tumor cells was performed by HMI. In contrast to conventional fluorescent microscopy, HMI systems can record the entire emission spectra of a fluorochrome in a single pass under the microscope. Each pixel in a scanned image radiates in more than 365-nm wavelengths and the HMI acquires the complete emission spectrum for every pixel. Pixels in the current studies were 0.3 μm in size. For each pixel, the emission spectrum was acquired followed by processing of the data using a spectral deconvolution algorithm. The deconvoluted signal attributable to each dye that is proportional to the amount of molecular marker expression is then presented for viewing with artificial colors designed to mimic those observed using conventional microscopy. These can then be viewed individually, or as overlays, and an inspection of these views enables the users to characterize the expression level following traditional (subjective, 0 to 3+) methods. A software package fits each pixel in a scanned image to a library of emission spectra for every fluorochrome. A spectrograph and computer analysis results in the separation and precise quantification of each fluorochrome despite overlapping emission spectra. For our purposes, HMI evaluates fluorescent antibody-based conjugates. Each conjugate represents an antibody to a different molecular marker, which is conjugated to a different fluorochrome. Therefore, the amount of the fluorescence intensity of each conjugate bound to the tumor cell gives a value for the level of expression of that molecular marker. A linear relationship exists between the fluorescence intensity value and the amount of protein measured. The number of molecules of a fluorochrome conjugated to an antibody is measured readily. Thus, software adjustments can be made for different batches of the same conjugate that have different average numbers of the same fluorochrome. Each fluorescent conjugate was used by itself or as part of a 10-tumor marker multiplex

to stain touch preps. The multiplex was considered complete only after the final results showed virtually identical values indicating no steric hindrance (or any other effect of the multiplex on expression of the individual conjugate).

HMI system and operation. The HMI system is composed of an Olympus IX-70 inverted microscope (Olympus, Center Valley, Pa), SP-500i imaging spectrograph (Acton Instruments Acton Research Corporation, Acton, Mass), Quantix KAF1600 charge-coupled device (CCD) camera (Photometrics, Tucson, Ariz), and X-Y motorized stage (Ludl Electronic Products Ltd, Hawthorne, NY). [8-11]

The movement of the stage and acquisitions of the camera are controlled by in-house VC++ programmed software running on a personal computer with the Windows XP operating system (Microsoft Inc, Redmond, Wash). The system records the full spectrum of a line of pixels from the sample image and moves the stage to the next line based on the slit width of the spectrograph and the objective power of the microscope. A microscope filter cube is used to excite the samples with 290 nm to 480 nm lamp radiation and permits the long pass of 420 nm and higher radiation emitted by the sample to reach the spectrograph's entrance slit. A 60× objective is used for cell scanning. The spectrometer grating (150 grooves per mm) and CCD array size (1536 × 1024 pixels of size 9 μm × 9 μm) enables a spectral acquisition range from 420 nm to 785 nm for the scans.[8-10] This combination of a single excitation band and long pass emission band provide the HMI with the novel capability to collect highly accurate continuous emission spectra. The entrance slit of the imaging spectrograph is coupled to the slide port of the microscope, and the CCD camera is mounted on the exit port of the spectrograph. The spectrum of the sample is focused on the CCD array, and thus, the irradiance intensity at the sample is also the intensity received at the CCD array.

The spectrometer entrance slit, set at 72 μm wide, views a width of the sample of 1.2 μm with a 60× objective and a length of 233.3 μm (14-mm long slit). Thus, each acquisition of the CCD camera will record the spectra radiating from a 1.2-μm width and cover a spatial length of 233.3 μm. The data presented used a 60x magnification such that each camera pixel represents 0.3 μm by 0.3 μm (2 × 2 binning). The spatial resolution along the slit length is set by the magnification and camera pixel size, whereas the perpendicular spatial resolution is set by the slit width. Spatial resolution can be improved by reducing the slit width.[8]

The HMI data acquisition sequence begins with the operator using a joystick to move the slide around above the microscope objective and optically select each cell for imaging. The cell is then scanned automatically. The spectra from 1 line crossing the sample at a time are recorded by the CCD camera, downloaded, and stored on the computer. The stage is controlled to move 1 imaged-slit-width at a time. The stage is stepped and spectra are recorded until the sample has been moved the full scan distance. A full scan sequence records on the computer hard drive an image cube of data consisting of spectral images. The image cube data are values which are 4-dimensionally related; 2 spatial (plane of the cell), 1 wavelength, and 1 intensity vs wavelength.[8-11]

Data cube analysis. Data cube files are transferred to other computers for analysis because the analysis software is independent of the acquisition software. Each 2-dimensional (2D) image of the spectra is integrated along the wavelength axis to give a line of intensity-varied pixels. The lines of pixels can be displayed adjacently in a picture to show a composite image of the scanned sample. But, more importantly, the image cube data are analyzed for spectral content.

The analysis programming is written in ITT Visual Information Solutions' Interactive Data Language (IDL). The analysis package begins with a graphical user interface for selecting the image cube of interest.[11] Next, the number and type of fluorochromes for deconvolution are selected through another graphical user interface. Then, the user is provided with the composite image, as described previously, to select interactively the region of interest that contains the cell or cells for analysis.

The software uses the IDL Curve_Fit function to determine the best least squares fit of a user-defined linear combination of the 11 spectra; 10 fluorochrome standards from the library and 1 background spectrum. The output is the set of coefficients for each standard spectrum that indicates the relative amount of each fluorochrome standard in the data spectrum.[11] Next, these best-fit coefficients for each marker are processed with the IDL WaterShed function to use its segmentation results to separate marker valves from background values. The final cell boundaries are determined from these results, and the cell morphology parameters are calculated. The average intensity for each marker is calculated by summing all the segmented coefficient values of a particular marker inside the cell boundary and dividing by the cell area. The marker values are also used to determine total marker intensity and marker pixels in the cell above a threshold. The marker data for each cell is saved in a 32-bit floating point Tagged Image File Format.

Figure 1 provides a representative sample of fluorescing spectra emitted from a 10-marker stained MCF7

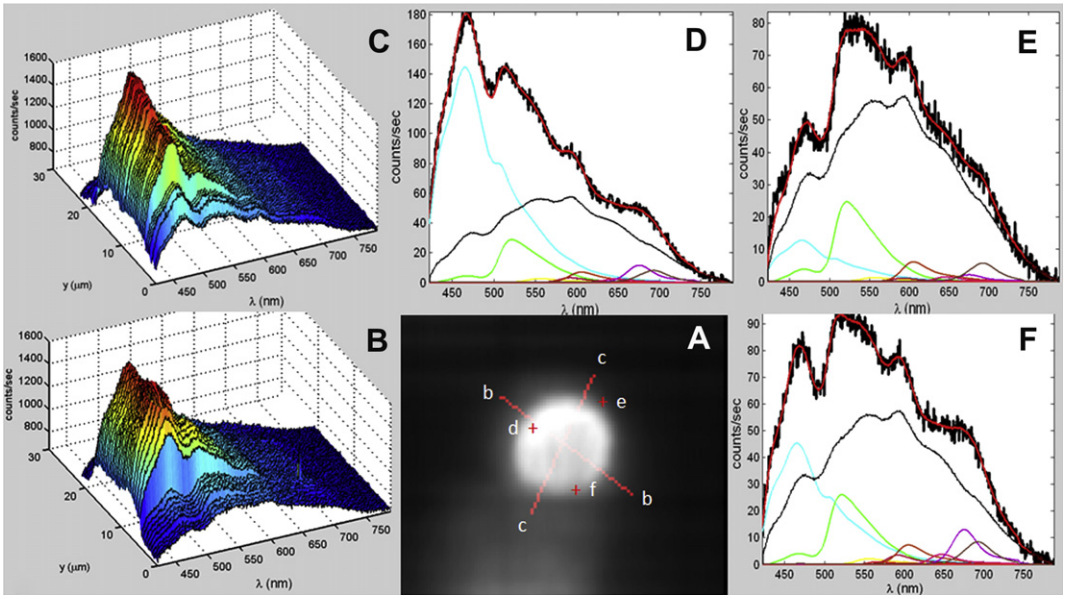

Fig 1. Representative sample of fluorescent spectra emitted from a 10-marker stained MCF7 cell. **A**, The wavelength integrated grayscale image of the cell which can be marked with lines to display a line of spectra (**B** and **C**) or individual points (**D, E**, and **F**). **B** and **C**, Graphic displays of interactively marked spatial lines in **A** of spectra corresponding to the data pixels along the lines b-b and c-c, respectively. **D–F**, The data spectrum (thick black) from individual pixels interactively marked by a "+" and labeled d, e, and f, respectively. Overlaid on the graphs are the standards (thin colors), background (thin black), and summation (thick red) curves derived during the analysis of the data spectra.

cell. Analysis software provides a wavelength-integrated grayscale 2D image of the cell (Fig 1, *A*), which can be queried interactively to display lines of spectra (Fig 1, *B and C*) or single-pixel spectra (Fig 1, *D–F*).[11] A line display provides the spectra along a spatial length of the image and is presented in a 3-dimensional (3D) graph format. The axes of the 3D graph are wavelength (λ) in nanometers, spatial (y) in microns, and intensity in counts/s. The software permits the scales to be varied and the coordinates system rotated. Single-pixel spectra are provided in 2D graphs but with overlays of the standard spectra used in the deconvolution and plotted proportional to their contribution to the total spectrum. The closely matching overlay of the sum (thick red) of all the standards (thin colors), including the background (thin black), onto the data spectrum (thick black) indicates the degree of accuracy in the deconvolution (Fig 1, *D–F*). Observing the number of the standard curves (thin colors) visible on a graph is a quick count of the number of markers present in that single pixel, as 9 of 10 are present in Fig 1, *F*.

Qualitative and quantitative analysis. An important correlative step allows us to display the cell for qualitative assessment by a certified pathologist from our team and other members of our Department of Pathology for quality control. Each marker value, as arrayed within the cell area, can be displayed separately or in combination. To assist in the assay, the markers can be false colored to match current pathology staining protocols and, especially when displayed in combinations, to distinguish 1 marker from another within the cell. The quantitative intensity values allow us to compare expression levels directly. In Figs 2 and 3, we show images of cell markers generated with the "cell average" method to represent the concentration levels with color intensity similar to that observed by pathologist for those fluors in the visible range.

In addition to spectral quantification, the analysis program computes 8 morphologic parameters simultaneously that are measured during analysis of each cell: These are cell area, cell perimeter, nuclear area to cell area ratio, cell long axis, cell short axis to long axis ratio, measured area to calculate ellipse area ratio, measured perimeter to calculated ellipse perimeter, and orientation angle. Graphs are made of average marker intensity and cell morphologic parameters.

Several HMI instruments have become commercially available (CitoViva Inc, LightForm Inc, Nikon Instruments Inc, etc) since we began to develop our HMI platform a decade ago.[12] To our knowledge, there are no published reports of quantification of a 10-color

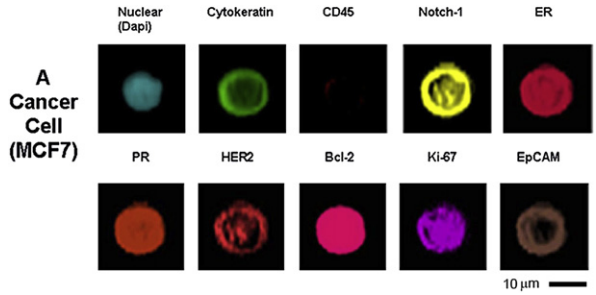

Fig 2. A 10-molecular-marker multiplex in a breast cancer cell line (MCF7). Each fluorochrome used in Fig 2 was attached to an antibody specific to a different molecular marker except for DAPI, which stains the nucleus directly. A representative cell is shown.

multiplex using one of these instruments. As described in Methods, there are many critical steps involving mechanics, microscopic, computer, and cellular analyses to accomplish a multicolor quantitative analysis.

Preparation of samples. Using polylysine-coated slides, touch preps of fresh breast cancer tissue were performed as described previously[13] or tumor cells (TCs) from cell lines were dropped gently onto slides and dried for 2 h at 37°C, then fixed for 10 min in ice cold acetone and stored at –80°C until stained. CTCs were captured from whole blood by an immunomagnetic assay as described previously.[14,15] Antibodies were obtained from Santa Cruz Biotechnology (Santa Cruz, Calif) and fluorochromes from Molecular Probes Inc (Eugene, Ore). Conjugation was performed according to the manufacturer's instructions. The TCs were stained with the conjugates, and the position of each TC on the slide was recorded by the microscopist examining the cytomorphology and the staining for cytokeratin and CD45. The ITCs were examined by HMI to determine the expression of each molecular marker. The TCs were stained with mouse monoclonal immunoglobulin G1 (IgG1), IgG2a, rabbit IgG, and goat IgG not specific to human antigens as negative controls. The specificity of each antibody conjugate was confirmed by analyzing reactions with appropriate cell lines with known expression levels for each molecular marker and with touch preps to ensure that both negative and positive results could be obtained. Two normal breast epithelial cell lines, which were recently established and characterized by Dr. David Euhus (University of Texas Southwestern Medical Center), were studied along with 5 neoplastic cell lines and clinical samples. The study conformed to the ethical guidelines for human and animal research. All human specimens were obtained after informed consent and were collected using protocols approved by the Institutional Review Board at the University of Texas Southwestern Medical Center, Dallas, TX.

Statistics. Statistical values were computed using the library functions provided in Microsoft Office Excel 2007. Error bars on graphs represent the ± 1 standard deviation of the mean. The R^2 value computed is the Pearson product moment correlation coefficient squared. Students t tests were used to compare the concordance of the 2 pathologists' subjective 0–3+ evaluations of the cell markers. Probabilities of $P < 0.05$ were considered significant.

RESULTS

The current study focused on the analysis of breast carcinoma as a prototype of cancer since analysis of molecular markers in breast cancer [eg, HER2, estrogen receptor (ER) and progesterone receptor (PR), etc] is a common approach in their evaluation by pathology and the levels of which affect treatment decisions for the patient.

We used touch preps to obtain ITCs on a slide rather than using routine paraffin embedded and formalin fixed tissue because the former improves analysis of cytomorphology. Fluorescent staining of touch preps allows the analysis of individual cells and facilitates the detection of nonrandom coexpression of specific molecular markers relevant to treatment decisions. Also, fluorescent staining identifies rare tumor cells such as putative cancer stem cells in a heterogeneous population. Ten different fluorochromes were used for each slide: 9 were conjugated to 9 different antibodies, each specific to a different molecular marker specifically selected for the analysis of breast cancer cells. One other fluorochrome, 4',6-diamidino-2-phenylindole (DAPI), stains the nucleus directly. The first aim was to quantify 10 molecular markers in a single pass of an ITC under the microscope. The development of this capacity to achieve a 10-tumor marker multiplex was complex because it was necessary to balance the intensity and background of the 10 different fluorochromes to decompose the spectral contributions of each fluor-antibody conjugate optimally.

Figure 2 shows the 10 molecular markers multiplex: nuclear, cytokeratin, cluster of differential 45 (CD45), Notch1, ER, PR, HER2, B-cell lymphoma 2, Ki-67, and epithelial cell adhesion molecule. The MCF7 breast cancer cell line was chosen as it is known to express all 9 markers (CD45 neg), each of which are significant in cancer biology or clinical decision making. In preliminary studies, we have evidence that additional complexes of antibody-fluorochrome conjugates can be constructed easily using this same wavelength-optimized set of fluorochromes by substituting 1 conjugate for another.

Initially, we quantified 10 molecular markers in 25 cells from 5 different cancer cell lines and 2 normal

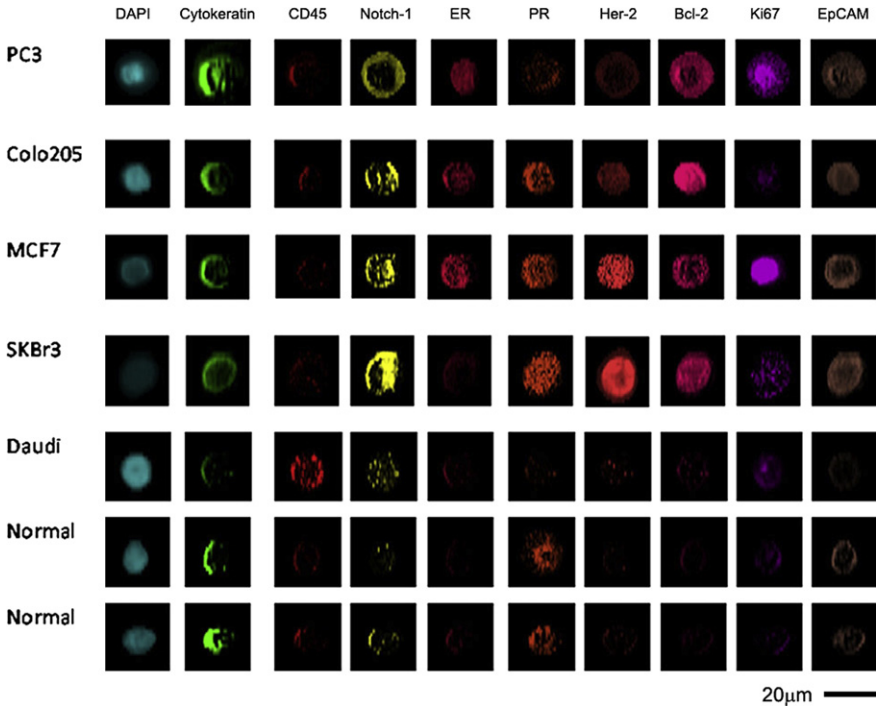

Fig 3. Ten immunofluorescence molecular markers were measured in 25 cells in 7 different cell lines. A representative cell from each cell line is shown. Cancer cell lines include SKBR3 and MCF from the breast; PC-3 from the prostate; Colo 205 from the colon; and Daudi from a B-cell lymphoma. Two normal breast epithelial cell lines are also shown. A single representative cell is shown for each cell line. Occasionally, the stain for a nuclear marker stains the cytoplasm for reasons that are not yet clear.

breast epithelial cell lines (providing 1700 measurements of tumor marker intensity). A representative cell was chosen from each cell line in Fig 3. This allowed us to obtain positive and negative controls for each conjugate. We showed previously that irrelevant immunoglobulins of the type used in the conjugates did not stain nonspecifically. This provided evidence that our results were concordant with those in the literature. In addition, it provided additional data on the extent of marker heterogeneity.

A visual examination of 25 TCs in a particular cell line showed a reproducible average tumor marker expression, although individual cells could vary substantially in expression of a particular molecular marker. As can be observed in Fig 3, the B cell lymphoma line Daudi expressed CD45 but not cytokeratin in contrast to the 4 carcinoma lines as expected. Also, the level of expression of markers on the cells of the 2 normal breast cell lines was markedly reduced compared to the cells of the 2 cancer cell lines: SKBr3 and MCF7.

We assessed the quantitative intensities output by the HMI for each molecular marker in tumor cells from clinical samples to correlate with the conventional pathologic analysis. Two authors (J.U. and H.L.) evaluated approximately 3000 cell images blinded to the nature of their source, including approximately 300 images that were inserted randomly in the set twice. These images were selected from the touch preps of 7 patients with breast cancer and from 5 patients with normal breasts or breasts containing benign tumors. The results showed that J.U. and H.L. had reproducibility errors of 15% and 20%, respectively. This was expected since this is a subjective analysis and the observer has to partition a very large range of image types and intensities into only 4 categories (0, 1+, 2+, and 3+), the scale typically used to categorize pathology samples. When we compared the results of the 2 observers, there was approximately 75% concordance. We then compared the averages of subjective 0–3+ analyses with that of the HMI analysis. Figure 4 shows a representative result with a highly significant Pearson correlation of 0.70, with a small standard error. We conclude that there is a general, but not a precise, concordance.

To evaluate tumor heterogeneity and reproducibility, we examined the number of tumor cells required to provide a "representative" quantification of the 10 molecular markers in a given cancer. There is no objective quantitative standard for reporting heterogeneity or variance in conventional pathologic analysis.[4,16] To approach this, we conducted 2 successive touch preps from a single breast cancer tumor from 11 different

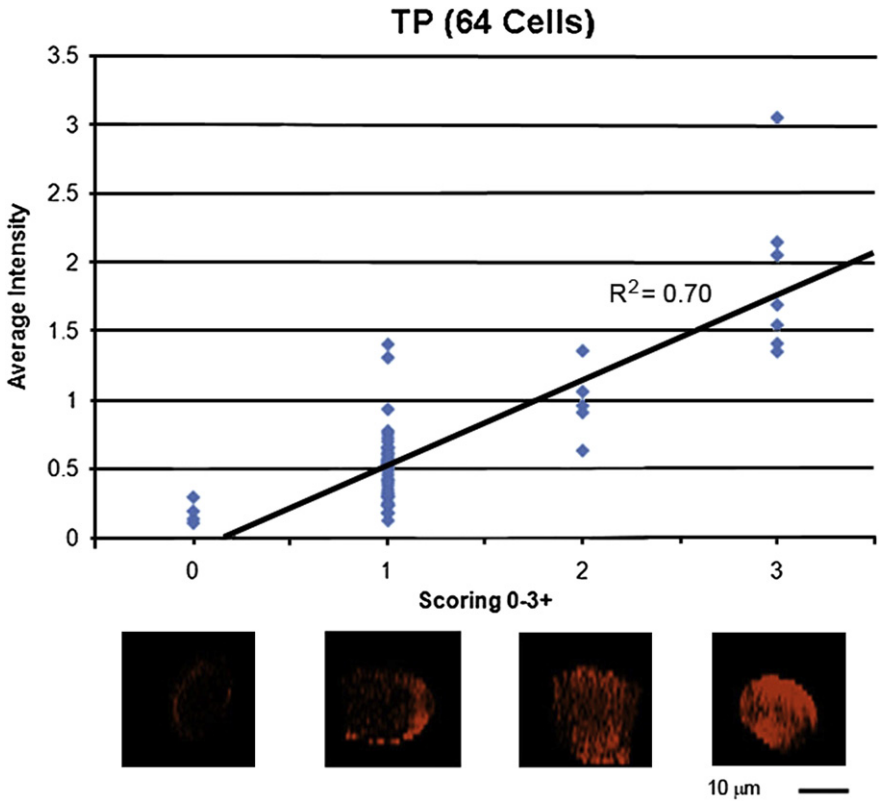

Fig 4. Comparison of average intensity determined by HMI analysis of 7 molecular markers to subjective conventional "human scoring" of 0–3+. The images at the bottom are a representative HER2 marker false color image of the respective subjective evaluation group 0–3+ plotted on the graph.

breast cancer patients. In this preliminary study, the HMI analysis of HER2 status matched the pathology report in 10 of 11 tissue samples taken at the time of breast tumor removal. Using our previous pattern, we examined 25 cells per touch prep for all 10 markers (5500 measurements). We compared the average intensity of molecular marker expression between the 2 touch preps. Figure 5 shows a representative experiment analyzing molecular markers from 2 touch preps from the same tumor. A marked heterogeneity was found, even though a comparison of the standard deviations of the average expression of each molecular marker showed no statistically significant differences between each other. This confirms that there is considerable heterogeneity among cancer cells but that the average levels of each of the 10 molecular markers from 25 TCs seems to provide representation of the tumor's molecular signature.

DISCUSSION

The major findings of this article are as follows: (1) A hyperspectral microscopic imaging platform was developed that can precisely quantify 10 molecular markers in a single pass of an individual TC; (2) touch preps of tumor tissue can be used to search for nonrandom patterns of molecular marker expression in ITCs that indicate clinical bias and could lead to new hypotheses; (3) HMI analysis of 25 TCs in a touch prep gave a defined molecular signature despite considerable heterogeneity within each molecular marker assay; and (4) HMI values of particular molecular markers were shown to correlate with the conventional $0–3^+$ subjective pathology analysis.

The claim of a "representative" analysis of a breast carcinoma by examining 25 TCs requires explanation. Using published data from clinical pathology laboratories, it is not possible to define "representative" in precise quantitative terms. There is significant heterogeneity within a given tumor,[16] and a subjective analysis among different laboratories shows considerable variability, eg. HER2, ER, and PR.[17,18] However, a comparison of the average intensities of the molecular markers from 2 touch preps from the same tumor yielded relatively similar results despite considerable heterogeneity within a single touch prep. A reasonable correlation

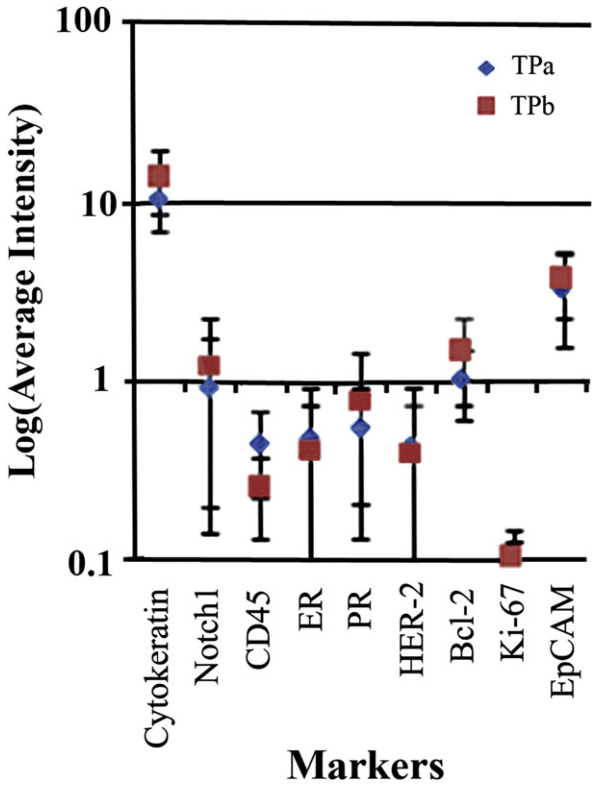

Fig 5. Two touch preps from a single patient. In all, 25 TCs were evaluated by HMI for 2 successive touch preps from the same biopsy. The average intensity and standard deviations are plotted.

was found between the HMI numbers and those obtained by standard pathologist examination using a 0–3+ analysis. This suggests that objective quantification has the potential to standardize analysis among different pathology laboratories provided the calculations for fluorescence expression were established for each tumor marker. The analysis is automated completely, and standardized instruments, procedures, and reagents are used. This will also require well-designed clinical correlative studies. However, once confirmed, there could be a major impact on standardizing the practice of reporting protein biomarkers and interlaboratory reproducibility.

The HMI analysis of ITCs adds to conventional pathologic analysis of molecular markers and to the vast repertoire of molecular assays currently under development for detection and quantification of both molecular markers and informative genes.[1-5,19-23] Currently, the amplification of the HER2 gene remains the gold standard for selecting patients for anti-HER2 therapy. This direct comparison of subjective observations of HER2 expression with the HMI evaluation provides an important potential tool. The precise and rapid quantification with the HMI generates values for each molecular marker that are reproducible and lack observer bias; thus, HMI may supplant current methodologies. Additionally, the baseline values generated from analysis at primary diagnosis can be compared with subsequent values either in cells obtained from metastatic sites or CTCs, not only impacting treatment strategies but also providing a deeper understanding of the evolutionary biology of the patient's tumor. For example, the analysis of individual breast cells from touch preps and CTCs indicated that 70% of HER2-amplified tumor cells had coamplification of the urokinase plasminogen activator receptor (uPAR) gene, significantly higher than the product of the individual frequencies of the amplification of each gene, which lies on different chromosomes.[24] We hypothesized that uPAR amplification might be essential for HER2-amplified cells to exert their increased malignancy. Several studies[24-26] support this hypothesis. Their data suggest that a targeting drug to inactivate uPAR together with trastuzumab may have a synergistic effect.[27,28]

Caution is warranted, however, before the application of HMI into routine clinical laboratory practice. Although the value generated by the HMI for each tumor marker in a particular cell is objective, extensive clinical validation studies must be done to determine which values will indicate their clinical significance. For example, a prospective validation study of patients with HER2+ tumors treated with trastuzumab using HMI and standard pathologic methods of HER2 analysis would be indicated to determine that the results generated by HMI define a biologically and clinically relevant status.

It is well known that tumors continue to evolve as they grow, progress, and metastasize. Each step in the progression of a tumor cell may be associated with additional genetic alterations and hence altered phenotypes. Continual phenotypic changes in cancer progression are a major obstacle to the individualization of treatment, particularly with regard to targeted therapy. It has been difficult to follow and document these changes and then harness the heterogeneity of tumors for effective treatment strategies because repeated invasive biopsies are not feasible.

It is also well known that significant heterogeneity can exist among metastases in a patient. Recently, because of the preceding reasons, there is considerable interest in characterizing CTCs. The development of various techniques and an automated instrument[5,29,30] that can count CTCs in recurrent breast, prostate, and colon cancer and thereby evaluate prognosis and efficacy of a treatment regimen has fueled recent attention and research in the field of CTCs. The evaluation of CTCs is now moving from mere enumeration of cells as

a prognostic indicator to expand the interrogation of the molecular signature, which encompasses the genetic and proteomic aspects of these cells. A provocative example is the acquisition of HER2 overexpression and gene amplification in CTCs in breast cancer progression.[13,30-34] Such patients may be candidates for treatment with anti-HER2 therapy but would not have been treated based on a negative primary tumor assay.

Conventional pathologic examination together with current fluorescence microscopy is insufficient to obtain the level of molecular profiling necessary to optimize new treatment regimens. HMI analysis of touch preps of tumor tissue and CTCs represents a major step forward because a large number of molecular markers can be detected and their expression precisely quantified in individual TCs. Eventually, this should have a positive effect on the prediction, prognosis, and prioritization of which targeting drugs should go into clinical trials. Coupled with extensive clinical experience, automation, standardization of HMI, and reagents, the exact values should replace subjective quantification and diminish or eliminate variation in results among different laboratories.

We thank Lisa Jones for help with the manuscript.

REFERENCES

1. Perou CM, Sorlie T, Eisen MB, et al. Molecular portraits of human breast tumors. Nature 2000;406:747–52.
2. Beske OE, Goldbard S. High-throughput cell analysis using multiplexed array technologies. Drug Discov Today 2002;7:S131–5.
3. Rennstam K, Hedenfalk I. High-throughput genomic technology in research and clinical management of breast cancer. Molecular signatures of progression from benign epithelium to metastatic breast cancer. Breast Cancer Res 2006;8:213–7.
4. Van de Vijver MJ, He YD, van't Veer LJ, et al. A gene-expression signature as a predictor of survival in breast cancer. N Engl J Med 2002;347:1999–2009.
5. Cristofanilli M, Budd T, Ellis M, et al. Circulating tumor cells, disease progression, and survival in metastatic breast cancer. N Engl J Med 2004;351:781–91.
6. Slamon DJ, Clark GM, Wong SG, et al. Human breast cancer: correlation of relapse and survival with amplification of the HER-2/neu oncogene. Science 1987;235:177–82.
7. Romond EH, Perez EA, Bryant J, et al. Trastuzumab plus adjuvant chemotherapy for operable HER2-positive breast cancer. N Engl J Med 2005;353:1673–84.
8. Huebschman ML, Schultz RA, Garner HR. Characteristics and capabilities of the hyperspectral imaging microscope. IEEE Eng Bio Med 2000;21:104–17.
9. Schultz RA, Nielsen T, Zavaleta JR, et al. hyperspectral imaging: a novel approach for microscopic analysis. Cytometry 2001;43:239–47.
10. Huebschman ML, Schultz RA, Garner HR. Hyperspectral imaging, review chapter, encyclopedia of modern optics. Waltham, Mass: Academic Press, 2004.
11. Huebschman ML, Rossenblatt KP, Garner HR. Hyperspectral microscopy imaging to analyze pathology samples with multi-colors reduces time and cost. Proc SPIE 2009;7182. 1F-1–10.
12. Garner HR, inventor; Board of Regents, The University of Texas System, assignee. Hyperspectral slide reader. U.S. patent 6,160,618. December 12, 2000.
13. Meng SD, Tripathy D, Shete S, et al. HER-2 gene amplification can be acquired as breast cancer progresses. Proc Natl Acad Sci U S A 2004;101:9393–8.
14. Fehm T, Solomayer EF, Meng S, et al. Methods for isolating circulating epithelial cells and criteria for their classification as carcinoma cells. Cytotherapy 2005;7:171–85.
15. Meng S, Tripathy D, Frenkel E, et al. Circulating tumor cells in patients with breast cancer dormancy. Clin Cancer Res 2004;10:8152–62.
16. Shipitsin M, Campbell LL, Argani P, et al. Molecular definition of breast tumor heterogeneity. Cancer Cell 2007;3:259–73.
17. Oyama T, Ishikawa Y, Hayashi M, Arihiro K, Horiguchi J. The effects of fixation, processing and evaluation criteria on immunohistochemical detection of hormone receptors in breast cancer. Breast Cancer 2007;14:182–8.
18. Wasielewski R, Hasselmann S, Rüschoff J, Fisseler-Eckhoff A, Kreipe H. Proficiency testing of immunohistochemical biomarker assays in breast cancer. Virchows Arch 2008;453:537–43.
19. Petricoin EF III, Bichsel VE, Calvert VS, et al. Mapping molecular networks using proteomics: a vision for patient-tailored combination therapy. J Clin Onc 2005;23:3614–21.
20. Ntoulia M, Stathopoulou A, Ignatiadis M, et al. Detection of mammaglobin A-mRNA-positive circulating tumor cells in peripheral blood of patients with operable breast cancer with nested RT-PCR. Clin Biochem 2006;39:879–87.
21. Piechev M, Naijer AJ, Pereira D, et al. Expression of VEGFR-2 and AC133 b circulating human CD identifies a population of functional endothelial precursors. Blood 2000;95:952–8.
22. Yow H, Wong JM, Chen HS, et al. Increased in mRNA expression of a-laminin binding protein in human carcinoma: complete sequence of a full-length cDNA encoding protein. Proc Natl Acad Sci U S A 1988;85:6394–8.
23. Katz RL, He W, Khanna A, et al. Genetically abnormal circulating cells in lung cancer patients: an antigen-independent fluorescence in situ hybridization-based case—control study. Clin Cancer Res 2010;16:3976–87.
24. Meng S, Tripathy D, Shete S, et al. uPAR and HER-2 gene status in individual breast cancer cells from blood and tissues. Proc Natl Acad Sci U S A 2006;103:17361–5.
25. Urban P, Vuaroqueaux V, Labuhn M, et al. Increased expression of urokinase-type plasminogen activator mRNA determines adverse prognosis in ErbB2-positive primary breast cancer. J Clin Onc 2006;24:4245–53.
26. Li C, Cao S, Liu Z, Ye X, Chen L. Meng, S. RNAi-mediated down regulation of uPAR synergizes with targeting of HER2 through the ERK pathway in breast cancer cells. Int J Cancer 2010;127:1507–16.
27. Faltus T, Yuan J, Zimmer B, et al. Silencing of the HER2/neu gene by siRNA inhibits proliferation and induces apoptosis in HER2/neu-overxpressing breast cancer cells. Neoplasia 2004;6:786–95.
28. Yu J, Kane S, Wu J, et al. Mutation-specific antibodies for the detection of EGFR mutations in non-small-cell lung cancer. CCR 2009;15:3023–8.
29. Cristofanilli M, Mendelsohn J. Circulating tumor cells in breast cancer: advanced tools for "tailored" therapy? Proc Natl Acad Sci U S A 2006;103:17073–4.
30. Müller V, Hayes DF, Pantel K. Recent translational research: circulating tumor cells in breast cancer patients. Breast Cancer Res 2006;8:110–3.

31. Alix-Panabières C, Riethdorf S, Pantel K. Circulating tumor cells and bone marrow micrometastasis. Clin Cancer Res 2008;14: 5013–21.
32. Fehm T, Becker S, Duerr-Stoerzer S, et al. Determination of HER2 status using both serum HER2 levels and circulating tumor cells in patients with recurrent breast cancer whose primary tumor was HER2 negative or of unknown HER2 status. Breast Cancer Res 2007;9:R74.
33. Solomayer EF, Becker S, Pergola-Becker G, et al. Comparison of HER2 status between primary tumor and disseminated tumor cells in primary breast cancer patients. Breast Cancer Res Treat 2006; 98:179–84.
34. Pestrin M, Bessi S, Galardi F, et al. Correlation of HER2 status between primary tumors and corresponding circulating tumor cells in advanced breast cancer patients. Breast Cancer Res Treat 2009;118:523–30.